Effect of Multistep Processing Technique on the Formation of Micro-defects and Residual Stresses in Zirconia Dental Restorations

Zhao Jing, DDS, PhD,[1,2] Zhang Ke, MD,[2] Liu Yihong, DDS, PhD,[3] & Shen Zhijian, PhD[2]

[1] Department of Prosthodontics, Peking University School and Hospital of Stomatology, Beijing, P.R. China
[2] Department of Materials and Environmental Chemistry, Arrhenius Laboratory, Stockholm University, Stockholm, Sweden
[3] Department of General Dentistry, Peking University School and Hospital of Stomatology, Beijing, P.R. China

Abstract

Purpose: The clinical failures of zirconia dental restorations are often caused by extrinsic artifacts introduced by processing. The aim of this study was to investigate the micro-defects and residual stresses generated during the multistep process of zirconia dental restorations.

Materials and Methods: Thermal spray granulated 3Y-TZP powders were dry pressed by two tools exhibiting distinctly different Young's moduli, cold isostatic pressed (CIP-ed), and pressure-less fully sintered. The green bodies pressed by a stiff tool were treated with different procedures: direct milling (green milling) followed by fully sintering; half-sintering and milling (raw milling) with or without fully sintering; and fully sintering followed by grinding. The fully sintered 3Y-TZP crowns were clinically adjusted using both a diamond bur and SiC bur, respectively. Phase composition and microstructure of the pressed, milled, and ground surfaces were studied by XRD and SEM.

Results: Tetragonal phase was the main phase of all detected 3Y-TZP specimens. Excessive residual stresses introduced by raw milling and grinding were confirmed by a strained T (111) peak, monoclinic phase, and obviously changed $I(002)_t/I(200)_t$ ratio. The residual stresses would form a compressive stress layer, while it was too shallow to inhibit crack propagation even for ground specimens. Large voids with high-coordination numbers were the common packing micro-defects. Once formed, they were barely healed by CIP-ing and sintering. A stiff pressing tool was confirmed to be useful for reducing the surface packing voids. Milling removed the surface voids, but was no help for the interior ones. Raw milling introduced more serious chippings, most originating from the existing packing voids, than green milling due to its brittle failure and was less recommended for production. Grinding dense 3Y-TZP caused surface grain refinement and much more severe micro-defects, especially when clinical adjustment was applied by diamond bur compared to SiC bur.

Conclusions: Micro-defects and residual stresses are introduced and accumulated through the entire production chain and determine the final microstructure of zirconia dental restorations. Several procedural improvements are offered and expected to reduce processing micro-defects.

Ceramics are increasingly used in dentistry due to their outstanding biocompatibility and esthetics. Particularly, 3 mol% yttria-stabilized tetragonal zirconia polycrystalline (3Y-TZP), as the strongest dental ceramic, is widely used to fabricate multiunit fixed partial dentures.[1] The excellent mechanical properties of 3Y-TZP originate from the stress-induced martensitic phase transformation from tetragonal to monoclinic symmetry.[2] During this phase transformation, a transformation zone develops around the growing crack, incrementally increasing the fracture toughness. A bending strength as high as 2 GPa has been reported in 3Y-TZP ceramics with added Al_2O_3.[3]

In practice, however, such excellent mechanical performance can rarely be achieved. Some 3Y-TZP frameworks fail after a short period, although this problem is always masked by porcelain chippings.[4-6] Since full-contour zirconia restorations generate much more interest today, the 3Y-TZP framework

reliability becomes more important. It has been well accepted in the ceramic field that micro-defects introduced during the production process were responsible for the decrease in fracture strength.[7] Although zirconia ceramics can benefit from phase transformation toughening, this mechanism becomes less effective at the weak parts of the restorations where micro-defects and residual stress are concentrated, like the cervical margin and the connections. Thus, it is necessary to understand and control the processing micro-defects and residual stress generated during zirconia restoration production.

The established production sequence of 3Y-TZP frameworks or full-contour restorations usually involves several steps: (1) green body formation by uniaxial dry pressing and/or cold isostatic pressing (CIP-ing) of powder granules; (2) computer-guided milling of porous blocks in green or half-sintered stage, denoted as green milling and raw milling, respectively; (3) sintering to fully dense; and (4) clinical adjustment by dentists or dental technicians through grinding, abrasion, and polishing. In previous studies, efforts have mainly been made to examine the effects of those preparation steps immediately close to clinical operation, for example, surface treatments on the performance of 3Y-TZP.[8-11] To date, few studies have considered the early part of the production chain and tried to illustrate the effect of the accumulated micro-defects and residual stresses through the entire production on the final microstructure and behaviors of 3Y-TZP restorations.

In this study, we investigated the micro-defects and residual stresses generated during processing steps and the evolution of the microstructure, which would determine the final properties of zirconia restorations. By correlating the characteristic micro-defects and residual stresses to certain manufacturing steps, this work ought to lead to safe preparation of and preventive measures for zirconia restorations.

Materials and methods

Specimen preparation

Commercial thermal spray granulated 3Y-TZP powders (Tosoh, Yamaguchi, Japan) were uniaxially pressed under 30 MPa with two different pressing tools, followed by CIP-ing under 200 MPa. The soft pressing tool exhibiting low Young's modulus (1 GPa) was made from gypsum-based hybrid material, and the stiff one with a high Young's modulus (200 GPa) was stainless steel. After fully sintering, two as-sintered specimens were made, labeled as LS (pressed by soft tool) and HS (pressed by stiff tool). Three groups of specimens with different densities were prepared by sintering the stiff tool pressed green bodies with different programs. The relative densities of green bodies without sintering, half-sintered bodies sintered at 1100°C, and fully sintered bodies sintered at 1500°C were 51.9%, 53.9%, and 98.3%, respectively. For different bodies, various surface finishing and heat treatments were applied as practical processes. Green bodies were green milled and then fully sintered (GmS). Half-sintered bodies were raw milled followed by fully sintering (RmS) or not (Rm). Feed speed for green milling and raw milling was 2.5 to 5 m/min and 1.5 to 2.5 m/min, respectively. Their tool rotating speed was ∼24 m/s for both. Clinically adjusted specimens (CA) were prepared by grinding the fully dense 3Y-TZP crowns using a high-speed

Table 1 Abbreviations of all experimental groups with different surface treatments

Abbreviation	Surface treatments[a]
LS	Green body (L) + fully sintered
HS	Green body (H) + fully sintered
GmS	Green body (H) + green milled + fully sintered
Rm	Green body (H) + half-sintered + raw milled
RmS	Green body (H) + half-sintered + raw milled + fully sintered
G	Green body (H) + fully sintered + ground
CA	Green body (H) + fully sintered + clinical adjusted

[a]Green body (L) was the green body compacted with soft tool; meanwhile, Green body (H) was the one compacted with stiff tool.

handpiece at 300,000 rpm under water cooling.[12] Two types of burs were applied, 80 μm diamond bur (MANI, Tochigi, Japan) and SiC bur (Dura-Green stones; Shofu, Kyoto, Japan). Grinding fully sintered bodies (G) were made as reference, and a grinding wheel with diamonds of 106 to 125 μm (ASTM standard E11 126/140) was used at a speed of 28 m/s. Except both CA and LS groups, which had only 3 specimens for microstructure observation, there were 10 specimens in the other 5 groups. The abbreviations of all experimental groups with different surface treatments are listed in Table 1.

Characterizations

The phase compositions were characterized with X-ray diffraction (XRD, X'Pert PRO; PANalytical, Almelo, the Netherlands) using Cu-Kα1 radiation ($\lambda = 1.5406$ Å). Scans were performed from 20° to 80° (2θ range) with a step size of 0.026° at 3° per minute. Clinically adjusted specimens were not analyzed due to their curved surfaces. I(002)$_t$/I(200)$_t$ ratio, the relative amount of monoclinic phase (Xm), and the relative thickness of surface phase transitions (TZD) were calculated according to the formulas proposed by Kosmač et al.[13]

For better observation of the surface features, all specimens were mildly acid etched by autoclaving in a mixed solution of phosphoric acid (H$_3$PO$_4$, 1.5 mol/L) and potassium chloride (KCl, 1 mol/L) under isothermal conditions at 200°C for 2 hours, except raw milled specimens, for which 2-hour etching was so severe that the original surface features were masked by a thick reaction product layer. Therefore, a 0.5-hour etching time was used instead for Rm and RmS. All specimens were cleaned ultrasonically with distilled water for 5 minutes, carbon coated, and investigated by scanning electron microscope (SEM, JEOL JSM-7000F; JEOL, Tokyo, Japan). Cross-section polishing (CP, SM-09010; JEOL) was used to analyze the micro-defects inside the ceramic bulk.

Results

XRD patterns are shown in Figure 1. The tetragonal phase was the main phase for all detected specimens, sometimes combined with a small amount of monoclinic phase. A sharp T(111) peak observed in specimens HS, GmS, and RmS indicated the high crystallinity of the tetragonal phase, whereas the broadening of the very same peak observed in specimens Rm and G disclosed
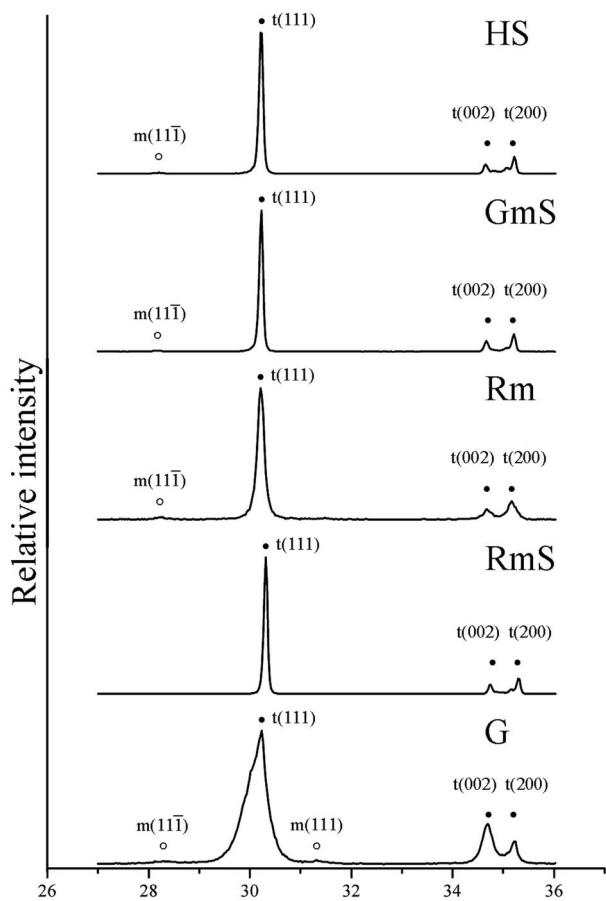
Figure 1 XRD patterns of 3Y-TZP specimens with different treatments, detected before acid etching.

Table 2 Mean values of $I(002)_t/I(200)_t$ ratios, relative amounts of monoclinic phase (Xm), and transformation depth (TZD) of 3Y-TZP with different surface treatments

	HS	GmS	Rm	RmS	G
$I(002)_t/I(200)_t$	0.56	0.63	0.56	0.62	1.73
Xm (mol%)	1.00	0.89	1.95	0	5.82
TZD (μm)	0.020	0.018	0.040	0	0.121

the high strain introduced by raw milling and grinding. The calculated $I(002)_t/I(200)_t$ ratio, Xm, and TZD are listed in Table 2. Especially for specimen G, the maximum Xm and TZD were observed and $I(002)_t/I(200)_t$ ratio changed reversely.

Figure 2 shows SEM micrographs of as-sintered specimens. Two kinds of voids can be distinguished, namely, intragranular and intergranular voids (Figs 2A, B). The former, in the fewer tens of nanometers range, was formed among individual particles softly aggregated together in every granule, whereas the latter, with two orders of magnitude larger size was formed among the packed granules with granule features still visible. On polished cross-section, the granule features became less obvious, yet the presence of two types of pores again appears characteristic (Fig 2C). Large pores with high-coordination numbers and
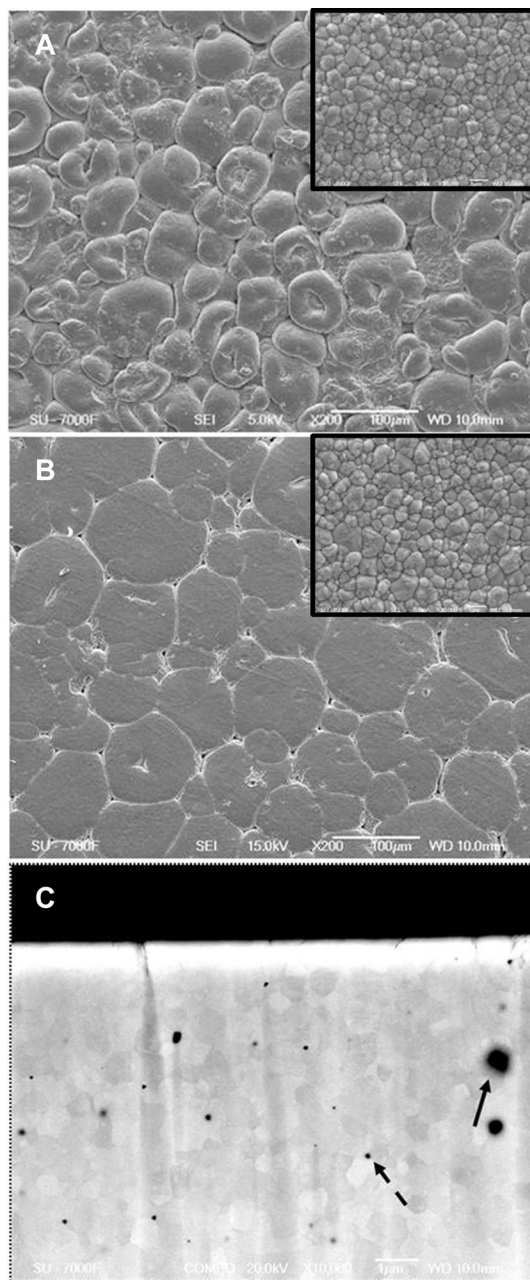
Figure 2 SEM micrographs of as-sintered specimens compacted with different tools: (A) LS and (B) HS, showing obvious heterogeneity of surface microstructures at low magnification. The inserted micrographs in (A) and (B) were taken at high magnification that show very similar features of close packing of 3Y-TZP grains on the pressed surfaces of LS and HS. (C) Cross-section view of HS, showing large pore (solid arrow) and small pore (dashed arrow) with high- and low-coordination numbers, respectively.

small pores with low-coordination numbers had their origins as intergranular and intragranular voids, respectively. At high magnification, specimens compacted by different tools showed similar homogeneous microstructures with nearly dense packing of crystalline grains of 0.3 to 1 μm (inserts in Figs 2A and B); however, the different inhomogeneous microstructures
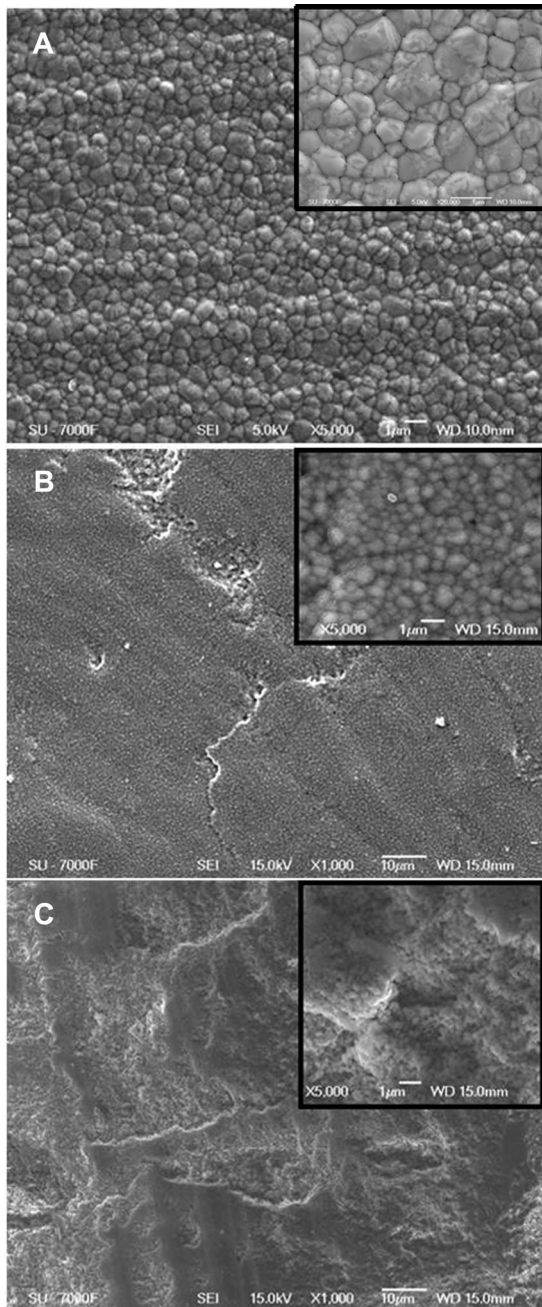
Figure 3 SEM micrographs of milled specimens: (A) the surface of GmS with no obvious defects. (B) Rm and (C) RmS, showing cracks and chippings formed after milling that remained after sintering. Micrographs with higher magnification are shown as inserts.

were visible at low magnification (Figs 2A and B). On the LS surface, the granules of 50 to 80 μm did not even change their spherical and/or doughnut morphologies, whereas on the HS surface, the granules were deformed, leaving packing void behind.

Figure 3 shows the SEM micrographs of the milled specimens. No obvious micro-defects were observed on GmS (Fig 3A), whereas more serious micro-defects appeared for Rm

and RmS (Figs 3B and C). Cracks and large areas of irregular chippings in the scale of tens of microns were the characteristic features of these raw milled surfaces.

Figure 4 shows the SEM micrographs of the ground specimens. Uneven microcracks, grain pullouts, and severe chippings were the common ground micro-defects. Through the large chippings, the original grains with the grain size in a range of 300 to 500 nm and a layer of "smashed grains" with a much smaller size, around 100 nm, were revealed (Fig 4B). Severe subsurface cracks formed along the grain boundaries were exposed by CP (Figs 4C and D). The thickness of this delaminating-like damage layer was about 3 μm. Many more chippings and deep grinding traces were formed on the CA surfaces (Figs 4E-H), especially when a diamond bur was used. Large chippings (about 30 μm) were observed on the diamond-adjusted surface (Fig 4E), whereas microcracks perpendicular to the grinding traces, with ~2 μm in length and 2 μm inter-spaces, were left on the SiC-adjusted surface (Fig 4H).

Discussion

Packing micro-defects and residual stresses

A dry-pressing process is commonly applied for the preparation of porous zirconia blocks. In this study, the common presence of intragranular and intergranular voids formed by packing of powder granules was confirmed,[14,15] indicating that homogeneous packing cannot be easily achieved, although the 3Y-TZP powders have been thermal spray granulated to improve the powder flowability and packing homogeneity. Once these voids formed, they are difficult to heal completely. On the one hand, deformation and breaking of granules by CIP-ing cannot remove all voids and particularly not change the wide size distribution of the remaining voids. On the other hand, sintering cannot eliminate the larger voids with high-coordination numbers either, and the high-temperature sintering unavoidably leads to grain growth.[16] At high temperatures, locally connected small pores may undergo pore coalescence to generate larger pores that will become the critical flaws.[17] For these as-sintered specimens, not so much transformation from tetragonal to monoclinic phase occurred. It indicates that seldom, residual stresses are generated by directly sintering the green bodies, and the compressive stress layer is too shallow to inhibit the crack propagation effectively.

The common micropictures of commercial zirconia products given by the manufacturers always show very similar dense grain packing; however, their features observed at low magnification are obviously different. It might be ascribed to the pressing tools, since to our knowledge, the pressing instruments and programs applied most often are similar and might not have as much of an effect on the formation of the surface features. Thus, two pressing tools with different moduli were applied, and this hypothesis was verified. The different surface microstructures of LS and HS indicate that the stiff pressing tool can effectively deform the granules and decrease the probability of large intergranular voids. Therefore, the use of a stiff pressing tool benefits the formation of a finer and denser surface with fewer packing micro-defects.
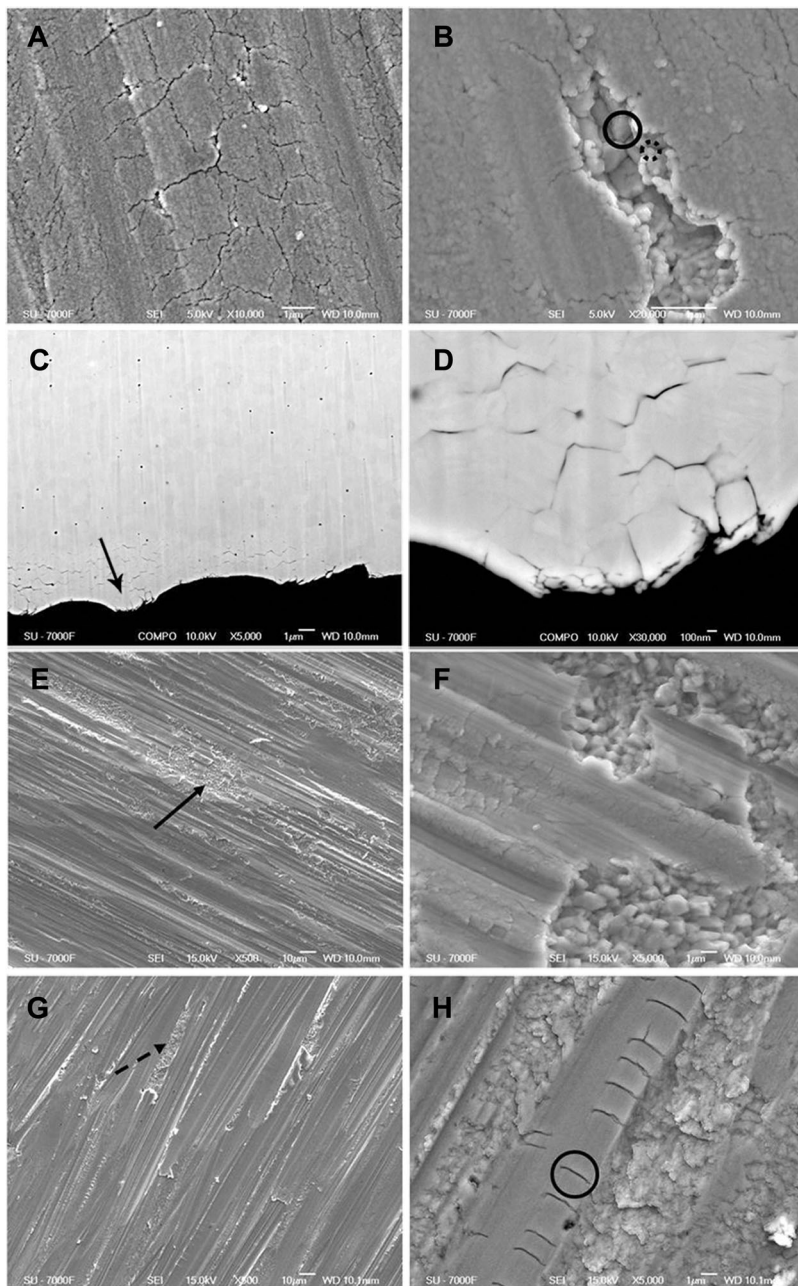
Figure 4 SEM micrographs of ground specimens: (A)–(D) and (E)–(H) showing microstructures of G and CA, respectively. (A) General microstructures of the surface of G. (B) As-sintered grains of micron size (solid circle) and small grains of nano size (dashed circle) inside the chippings on the surface of G. (C) Cross-section view highlighting a delaminating-like damage layer and local morphology (arrow) with high magnification in (D). Surface microstructures of adjusted dense 3Y-TZP by diamond bur (E) and by SiC bur (G). (F) and (H) exposing local features of the marked area in (E) and (G), respectively. Characteristic parallel cracks (solid circle) are shown in (H).

Milling micro-defects and residual stresses

With current technology, the complex geometries of dental restorations made of 3Y-TZP ceramics are generated by customized milling of porous blocks. During milling, surface materials are removed as are the surface micro-defects; however, there is no help to remove any interior packing micro-defects. Instead, the interior intergranular voids will be exposed to the surface by milling. They will seriously deteriorate the performances of 3Y-TZP restorations, especially when such defects are located at crucial positions of the restorations.[18] Besides exposition of preexisting micro-defects, milling also can introduce additional micro-defects and residual stresses. Based on

the findings of this study, green milling generated less residual stresses and fewer micro-defects than raw milling did, although it is not as popular as raw milling, especially in dental laboratories. This can be ascribed to the different milling mechanisms. For green milling, ductile deformation occurs at the initial stage, as organic binder exists to strengthen the very weak green body lacking strong interparticle connection. No further deformation is possible when the yield strength is approached, and local brittle failure as chippings would appear by further increase of the milling force. Thus, lower force is recommended for green milling to avoid severe chippings and excessive stresses. For raw milling, ductile deformation is impossible, because the organic binders have been completely burned off. Though

necks are formed between individual grains during sintering, these partially sintered porous bodies are typically brittle materials. Their local brittle failure has a very close relationship with the preexisting packing micro-defects. Materials would be removed along the large crack-like voids, which caused extremely rougher surfaces with serious cracks and chipping. In other words, the microstructure formed after raw milling is more sensitive to the quality of porous blocks than green milling. Although the stresses introduced by raw milling can be released by sintering, the micro-defects can hardly be healed.

Clinically adjusting micro-defects and residual stresses

Clinical adjustment of restorations is a common and important step applied by dentists or dental technicians through grinding fully dense 3Y-TZP restorations. The goals are to improve the fitting, to get the precise geometry, and to adjust the occlusal contacts. As clarified before, powder packing and green milling would not generate excessive residual stresses; however, grinding dense zirconia could. The broadened and strained T(111), monoclinic phase over 5 mol%, and the obviously reversed $I(002)_t/I(200)_t$ ratio supported the stress-induced phase transformation and the formation of residual stresses.[19,20] The surface compressive stress layer formed by residual stresses should be beneficial for strengthening; however, this 0.12 μm layer is still too shallow to withstand polishing and annealing treatments.[21]

Grinding micro-defects, that is, serious chippings and deep grinding traces, were exposed on the clinically adjusted fully dense 3Y-TZP restorations. It appears that these micro-defects are formed due to high and inhomogeneous forces applied by hand to remove the dense material.[22,23] In fact, their formations are originated and accelerated by the already existing packing and milling micro-defects inside. Grain refinement was observed in this study. It might be caused by mechanically breaking of the coalescence grains into initial small particles by excess local stresses and tends to increase the stability of the tetragonal phase.[24] The observed $\sim$3 μm delaminating-like damage layer is an indication of slow subcritical crack growth and surface hydrothermal degradation in the acidic environment.[25] The micro-defects and inhomogeneous stresses have been confirmed as the crucial factors for the LTD and fatigue resistant-properties of 3Y-TZP.[26] It indicates that especially when full-contour zirconia restorations are used, once the accumulative micro-defects and residual stresses generated during production procedures and presented within the restorations are directly exposed to the oral environment under occlusal forces, the reliability of 3Y-TZP restorations will deteriorate.

The importance of selection and application of grinding tools has been proposed previously, mainly regarding grit size and grinding parameters. In this study, the effect of grinding tool material on the formation of grinding micro-defects was clarified. Compared with SiC, more micro-defects formed when dense 3Y-TZP was ground by a harder and stiffer diamond bur because grit load was enlarged to generate a higher removal rate and more cracks.[22] Clinical adjustment, especially by hand with a stiff bur, should be minimized as much as possible. For

this purpose, the precision of 3Y-TZP restorations should be optimized, and the processing defects can be minimized during the early stages of the production processes.

Conclusions

Processing micro-defects and residual stresses are introduced during zirconia restoration production from industrial production, lab preparation, and to clinical adjustment. The micro-defects and residual stresses formed in each processing step are cumulative and determine the microstructure evolution and the final properties of 3Y-TZP restorations. To increase the strength and to ensure the reliability of 3Y-TZP restorations, caution should be taken (1) to decrease packing voids with high-coordination numbers by improving the quality of starting powder granules and/or by using a stiff tool for dry pressing; (2) to minimize milling micro-defects preferably by green milling with a relatively low force; and (3) to eliminate or reduce grinding micro-defects by avoiding clinical adjustment or using an SiC bur instead of a diamond bur.

Acknowledgments

References

1. Piconi C, Maccauro G: Zirconia as a ceramic biomaterial. Biomaterials 1999;20:1-25
2. Garvie RC, Hannink RH, Pascoe RT: Ceramic steel? Nature 1975;258:703-704
3. Tsukuma K, Ueda K, Shimada M: Strength and fracture-toughness of isostatically hot-pressed composites of Al_2O_3 and Y_2O_3-partially-stabilized ZrO_2. J Am Ceram Soc 1985;68:C4-C5
4. Sailer I, Feher A, Filser F, et al: Five-year clinical results of zirconia frameworks for posterior fixed partial dentures. Int J Prosthodont 2007;20:383-388
5. Ortorp A, Kihl ML, Carlsson GE: A 3-year retrospective and clinical follow-up study of zirconia single crowns performed in a private practice. J Dent 2009;37:731-736
6. Molin MK, Karlsson SL: Five-year clinical prospective evaluation of zirconia-based Denzir 3-unit FPDs. Int J Prosthodont 2008;21:223-227
7. Lange FF: Processing-related fracture origins: I, observations in sintered and isostatically hot-pressed Al_2O_3/ZrO_2 composites. J Am Ceram Soc 1983;66:396-398
8. Kosmač T, Oblak Č, Marion L: The effects of dental grinding and sandblasting on ageing and fatigue behavior of dental zirconia (Y-TZP) ceramics. J Eur Ceram Soc 2008;28: 1085-1090
9. Aboushelib MN, Wang H: Effect of surface treatment on flexural strength of zirconia bars. J Prosthet Dent 2010;104:98-104
10. Luthardt RG, Holzhuter M, Sandkuhl O, et al: Reliability and properties of ground Y-TZP-zirconia ceramics. J Dent Res 2002;81:487-491
11. Wang H, Aboushelib MN, Feilzer AJ: Strength influencing variables on CAD/CAM zirconia frameworks. Dent Mater 2008;24:633-638

12. Curtis AR, Wright AJ, Fleming GJP: The influence of surface modification techniques on the performance of a Y-TZP dental ceramic. J Dent 2006;34:195-206

13. Kosmač T, Oblak Č, Jevnikar P, et al: The effect of surface grinding and sandblasting on flexural strength and reliability of Y-TZP zirconia ceramic. Dent Mater 1999;15: 426-433

14. Galakchov AV, Shevchenko VJ: Influence of pore structure inhomogeneities in green compacts on strength and reliability of Y-TZP. J Eur Ceram Soc 1990;6:317-322

15. Adolfsson E, Shen ZJ: Effects of granule density on strength and granule related defects in zirconia. J Eur Ceram Soc 2012;32:2653-2659

16. Trunec M, Maca K: Compaction and pressureless sintering of zirconia nanoparticles. J Am Ceram Soc 2007;90: 2735-2740

17. Xiong Y, Hu JF, Shen ZJ, et al: Preparation of transparent nanoceramics by suppressing pore coalescence. J Am Ceram Soc 2011;94:4269-4273

18. Liu YH, Feng HL, Bao YW, et al: Fracture and interfacial delamination origins of bilayer ceramic composites for dental restorations. J Eur Ceram Soc 2010;30:1297-1305

19. Guess PC, Zhang Y, Kim JW, et al: Damage and Reliability of Y-TZP after Cementation Surface Treatment. J Dent Res 2010;89:592-596

20. Kondoh J: Origin of the hump on the left shoulder of the X-ray diffraction peaks observed in Y_2O_3-fully and partially stabilized ZrO_2. J Alloy Compd 2004;375:270-282

21. Kao HC, Ho FY, Yang CC, et al: Surface machining of fine-grain Y-TZP. J Eur Ceram Soc 2000;20:2447-2455

22. Yin L, Jahanmir S, Ives LK: Abrasive machining of porcelain and zirconia with a dental handpiece. Wear 2003;255:975-989

23. İşeri U, Özkurt Z, Kazazoğlu E, et al: Influence of grinding procedures on the flexural strength of zirconia ceramics. Braz Dent J 2010;21:528-532

24. Whalen PJ, Reidinger F, Antrim RF: Prevention of low-temperature surface transformation by surface recrystallization in yttria-doped tetragonal zirconia. J Am Ceram Soc 1989;72:319-321

25. Marro FG, Camposilvan E, Anglada M: Revealing crack profiles in polycrystalline tetragonal zirconia by ageing. J Eur Ceram Soc 2012;32:1541-1549

26. Kosmač T, Kocjan A: Ageing of dental zirconia ceramics. J Eur Ceram Soc 2012;32:2613-2622